Liquid crystal thermography on coated SAW devices

C. Huck, H. P. Zidek, T. Ebner, K. C. Wagner, Achim Wixforth

Angaben zur Veröffentlichung / Publication details:

Huck, C., H. P. Zidek, T. Ebner, K. C. Wagner, and Achim Wixforth. 2012. "Liquid crystal thermography on coated SAW devices." In *2012 IEEE International Ultrasonics Symposium, Dresden, Germany, 7-10 October 2012*, 2493–96. Piscataway, NJ: IEEE. https://doi.org/10.1109/ultsym.2012.0624.

10.1109/ULTSYM.2012.0624

Liquid Crystal Thermography on Coated SAW Devices

C. Huck[1,2], H. P. Zidek[2], T. Ebner[2], K. C. Wagner[2], and A. Wixforth[1]

[1] Institute of Physics, University of Augsburg, 86159 Augsburg, Germany
[2] TDK / EPCOS AG, 81671 Munich, Germany

***Abstract*—Reliability of micro-electronic devices is one of the most important issues in modern technologies and is significantly influenced by the thermal behavior of the components. In this context, we present Liquid Crystal Thermography (LCT) not only as an easy-to-use but even comparably low-cost approach for temperature measurements. This technique is based on thermochromic liquid crystals which exhibit temperature-dependent colors by selectively reflecting incident white light. We describe and demonstrate this method in exemplary investigations of self-heating effects in a half-section ladder-type Surface Acoustic Wave (SAW) filter with silicon dioxide coating. Conventionally, mean temperature values are obtained by evaluating measured frequency shifts under load by means of the Temperature Coefficient of Frequency (TCF). Moreover, LCT provides spatially resolved measurements of the temperature distribution on the component and serves as an independent scheme for thermal characterization in contrast to TCF based evaluations. The results of LCT measurements and temperature simulations are compared and show good agreement.**

I. Introduction

Modern UMTS and LTE mobile communication systems make high demands on RF filtering applications. Devices based on Surface Acoustic Wave (SAW) technology meet these requirements very well. However, despite many years of research and development, domains such as reliability and lifetime are still subject of current investigations and need to be thoroughly studied [1]. One of the important issues deteriorating the device reliability is the increase of internal temperature due to power dissipation in the component [2]. This so-called self-heating at high electrical power levels causes crucial frequency shifts of the filter characteristics especially since RF duplexer specifications demand small transition bandwidths and steep filter skirts. Therefore, investigating the temperature behavior of a SAW resonator is an important task regarding reliability considerations and is necessary to optimize the filter design.

A common method uses the frequency shift of the transfer function in order to determine the component's temperature indirectly. Variation of ambient temperature results in the Temperature Coefficient of Frequency (TCF) which serves as a quantity to map the frequency shift to an accurate value of the temperature increase. However, temperatures determined that way are attributed homogeneously to the entire chip without taking local inhomogeneities into account. Additional problems arise using this indirect approach as soon as other effects causing a frequency shift play a role. Hence, the study of temperature dependent effects necessitates a direct measurement method to precisely ascertain the device temperature.

[1] Corresponding author: christian.huck@physik.uni-augsburg.de

There are many different approaches for nondestructive temperature measurements available, physically contacting methods as well as noncontacting optical methods [3, 4]. For conventional uncoated SAW devices only noncontacting methods like Infrared Thermography (IRT) may be used, while their coated counterparts allow the application of contacting measurement techniques, too. Methods that rely on physically contacting the device include point contacting and multiple contacting realizations with blanket coatings, but all of them are based on a transfer of thermal energy from the device of interest to the object contacting the device, the thermometer. As we intend to measure the temperature distribution of the entire component, only multiple contacting approaches are considered. In this study, Liquid Crystal Thermography (LCT) is applied for thermal mapping of coated SAW devices under load. This is a popular technique in nondestructive testing of electronic devices and relies on Thermochromic Liquid Crystals (TLCs) which selectively reflect incident white light depending on their temperature [5–8].

Sec. II of this paper describes the experimental procedure including sample preparation, TLC calibration, measurement setup and evaluation process. In Sec. III temperature distributions obtained by LCT measurements and according simulations are presented. The respective results are compared and discussed in Sec. IV.

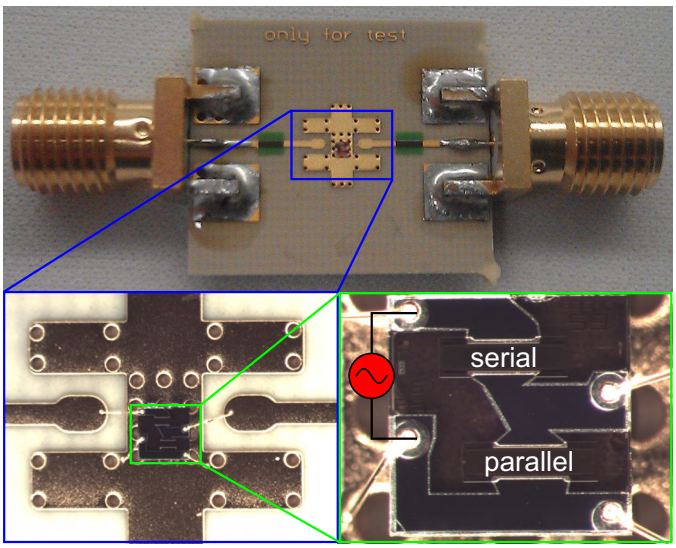

Fig. 1. The investigated device is a half-section ladder-type SAW filter with SiO_2 coating that consists of a serial and a parallel resonator with the former next to the input. It is mounted on a PCB by an epoxy adhesive.

II. Experimental Procedure

In the following, the experimental procedure for the thermal mapping of coated SAW devices using LCT is described. Before actually measuring the temperature distribution of the component under load the sample needs to be thoroughly prepared. For a quantitative temperature analysis calibration of the TLCs is mandatory.

A. Sample Preparation

In this study, we investigate a half-section ladder-type SAW filter which consists of one serial and one parallel resonator and is mounted on a PCB by an epoxy adhesive (see Fig. 1). The resonator surfaces are passivated with a thick temperature compensating SiO2 layer. This allows for contacting temperature measurements like LCT due to the negligible amplitude of the acoustic wave at the surface. For this purpose, two additional thin layers are deposited on the component's surface by an airbrush system. The first layer is a light absorbing black backing paint (Hallcrest SPB100) which offers improved optical analysis due to the well-defined background. The second layer is composed of micro-encapsulated TLCs with an active temperature bandwidth of 20 K starting at approximately 60°C (Hallcrest R60C20W). It serves as the actual temperature expressing layer.

B. Calibration of TLCs

Following the sample preparation the TLCs need to be calibrated to allow for an accurate quantitative temperature analysis as indicated in Fig. 3. Therefore, the illuminated Device Under Test (DUT) is heated homogeneously across its active temperature range using a hotplate. Simultaneously, a digital color camera takes snapshots through an optical microscope and a thermocouple measures the current temperature of the DUT. The camera provides RGB images which are transformed into HSV color space in order to enable a scalar color evaluation using hue values. The measured mean hue value of

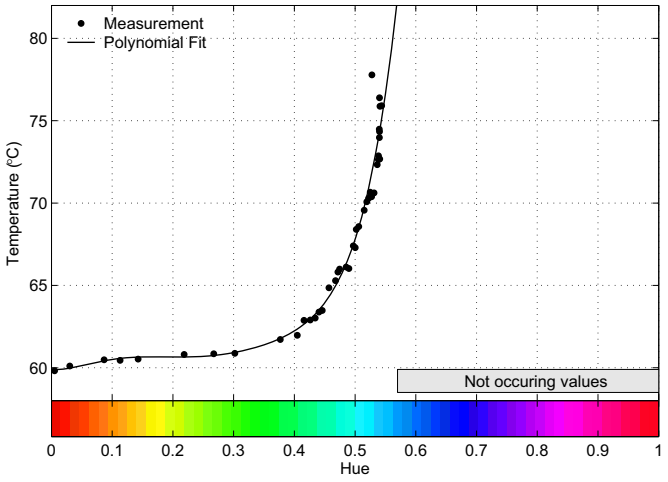

Fig. 2. TLC calibration by means of a sixth order polynomial fit to the data. It is used for post-processing of the self-heating measurements.

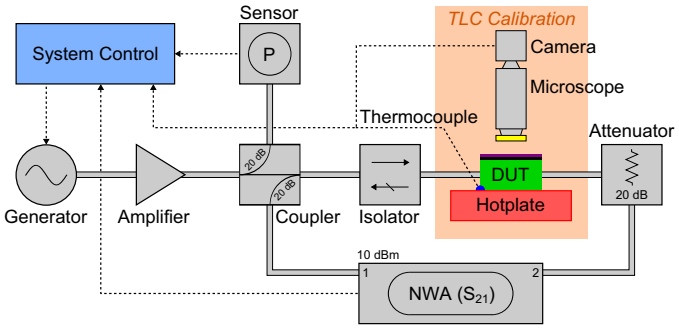

Fig. 3. Experimental setup for self-heating measurements with the relevant equipment for TLC calibration highlighted.

a predefined calibration area on the component as a function of temperature is shown in Fig. 2. A sixth order polynomial fit to this data serves as the TLC calibration in the actual self-heating measurements for post-processing of hue images in order to determine the corresponding temperature values. Details regarding image processing and calibration procedure as well as possible calibration errors like illumination and viewing arrangement or hysteresis and aging of TLCs are extensively discussed elsewhere [9–13].

C. Measurement Setup

The schematic in Fig. 3 illustrates the experimental setup used for self-heating measurements presented in this paper. The RF generator is connected to the power amplifier which feeds the DUT via a directional coupler. A power sensor detects the applied power and a Network Analyzer (NWA) measures the transfer function of the DUT. Protection of the NWA and the power amplifier is ensured by an attenuator and an isolator. The signal path and its frequency-dependent power attenuation is calibrated for all load frequencies. In order to raise the ambient temperature narrowly below the TLC's active temperature range the DUT is placed on a hotplate, the temperature of which is measured by a thermocouple. A digital color camera records the LCT color distribution on the illuminated DUT via a microscope and adjusts gain and exposure automatically for each image. The entire measurement setup is controlled by a LabVIEW program which sets load frequency and power at the RF generator and reads out the NWA, the power sensor, the thermocouple and the digital camera.

D. Evaluation Process

The recorded LCT color distribution images require post-processing to allow for an accurate temperature evaluation. On the one hand, hue values at every pixel need to be converted to temperature values using the aforementioned TLC calibration curve. On the other hand, corrections have to be applied due to uncolored pixels caused by imperfections in the TLC coating and reflective areas. While the latter is corrected by means of difference considerations based on a reference image without load, uncolored pixels are taken into account by truncated filtering of brightness values. The resulting thermal maps are presented in the following section.

III. Measurement and Simulation Results

In Fig. 4 qualitative temperature distributions of the DUT under load are visualized. The top panel illustrates raw LCT images at three different load frequencies, at the left skirt, at the passband center and at the right skirt of the filter. Since these images are not post-processed and converted to temperature values, they reveal the actual color distribution on the component's surface ranging from red to blue corresponding to approximately 60°C and 80°C, respectively (see Fig. 2). The central panel shows the associated post-processed LCT measurements after TLC calibration and brightness filtering. According FEM simulation results are depicted in the bottom panel. In detail, losses resulting from the simulated acoustic and electromagnetic energy fields are used to determine the temperature distribution. In this context, heat conduction and convection of the entire sample comprising chip, PCB, bondwires and epoxy adhesive are taken into account.

The right skirt of a half-section ladder-type filter is mainly dominated by the serial resonator, whereas the parallel resonator basically defines the left skirt. Hence, loading the filter at the upper edge of the transfer function, where the serial resonator is near to its antiresonance, particularly heats up the serial resonator. Due to the small power transfer the parallel resonator is only affected by heat conducted from the serial resonator.

Loading the filter at the left skirt or the passband center results in heating of both resonators because RF power is dissipated in both of them. By applying RF power at the lower

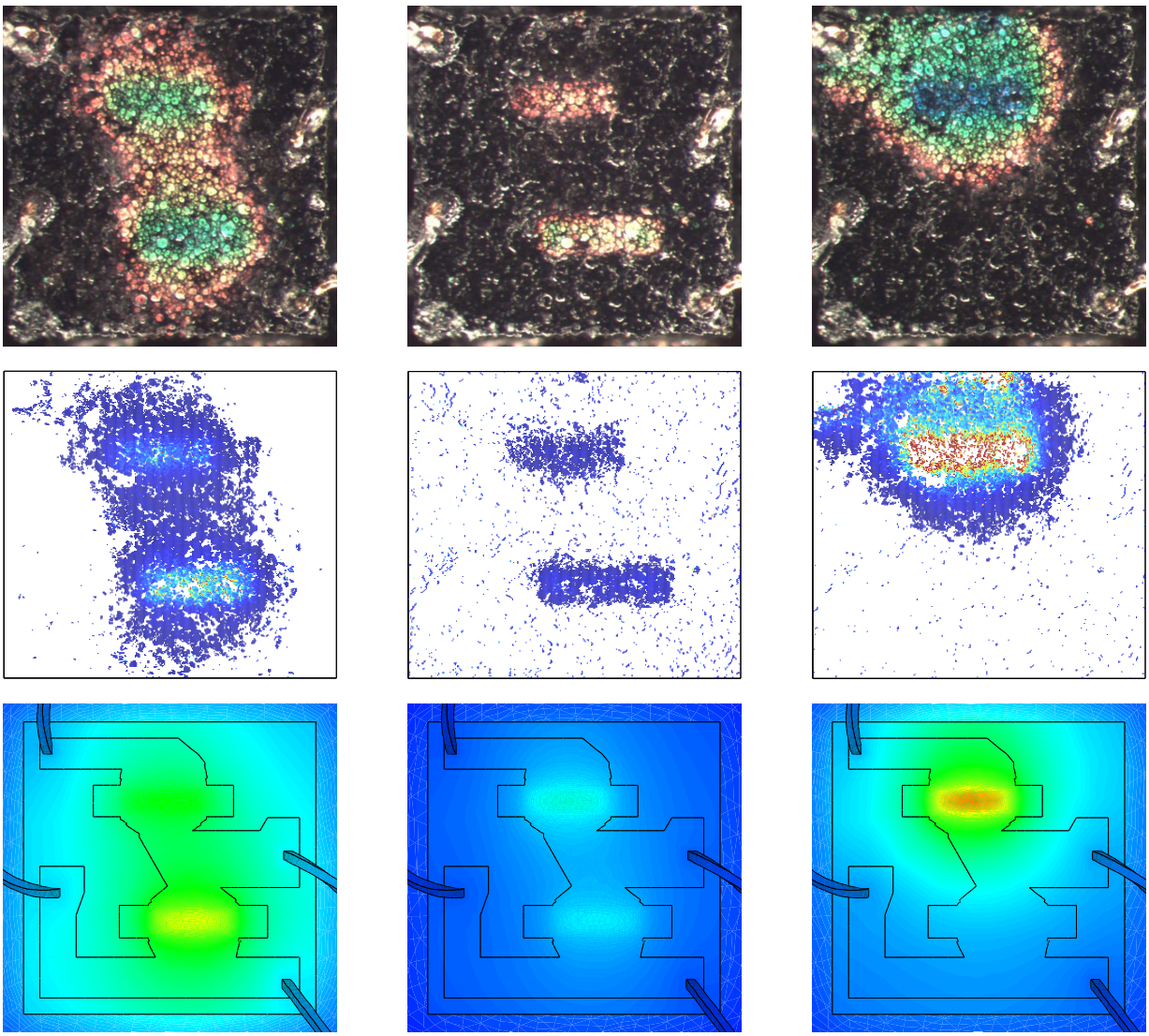

Left skirt at 890 MHz. Passband center at 930 MHz. Right skirt at 970 MHz.

Fig. 4. Measured (top panel), post-processed (central panel) and simulated (bottom panel) temperature distributions on a half-section ladder-type SAW filter with SiO_2 coating under load ($P = 25$ dBm). The measurement was performed with LCT, post-processing was conducted according to Sec. II-D and the simulation was performed with ANSYS. All are shown for three different load frequencies, at about the left skirt, at the passband center and near to the right skirt of the filter.

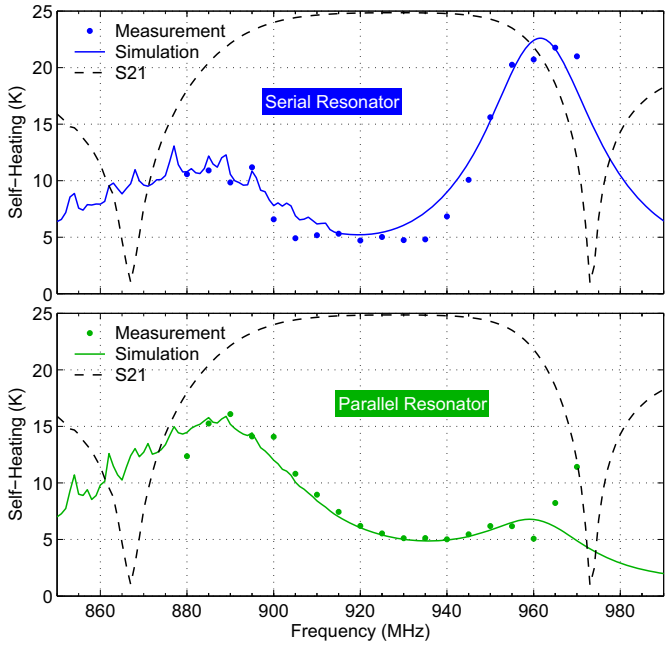

Fig. 5. Measured and simulated self-heating of the serial and parallel resonator in a half-section ladder-type SAW filter with SiO_2 coating as a function of load frequency at $P = 25\,\mathrm{dBm}$. The transfer function (S_{21}) of the filter is added as a reference in arbitrary units.

edge of the transfer function, where the parallel resonator is near to its resonance, the power transferred from the serial resonator is dissipated in the parallel resonator due to its lower impedance compared to the matched output.

At the passband center, near the serial resonator's resonance and the parallel resonator's antiresonance, neither is heated significantly. Due to the large impedance of the parallel resonator power passed through the serial resonator is mainly discharged at the load.

IV. Discussion

In Fig. 5 the self-heating of the serial and parallel resonator is analyzed quantitatively as a function of load frequency. The noticeable distortions below the resonance frequency of each resonator are caused by narrowband reflectivity variations due to improperly tuned reflectors. Using the maximum occuring temperature value defined by the TLC calibration the heat transfer coefficient in simulation is adjusted to fit the measurement. Thereby, good agreement between LCT measurement and simulation results is observed. At the right filter skirt deviations between measurement and simulation of the parallel resonator occur. They are explainable since the TLCs are below their active temperature range resulting in undefined hue values (see Fig. 4). This issue can be overcome by setting the hotplate's temperature within the TLC's active bandwidth.

Further investigations will include comparison with TCF based temperature evaluation and with unitarity violation which quantifies the entire power loss in the device. As an independent verification alternative noncontacting temperature measurement methods such as IRT and Raman Spectroscopy could be applied. While IRT enables measurements with a larger temperature range, the main advantage of the latter is its submicron spatial resolution.

V. Conclusion

In this work, we presented LCT as an easy-to-use and comparably low-cost alternative for temperature measurements. The technique is demonstrated in exemplary investigations of self-heating effects in a half-section ladder-type SAW filter with SiO_2 coating. On top of mean temperature values obtained by conventionally evaluating measured frequency shifts using TCF values, LCT provides spatially resolved measurements of the temperature distribution on the component. Moreover, LCT eliminates measurement uncertainties caused by other effects resulting in a frequency shift. In this regard, it serves as an independent measurement scheme unlike TCF based evaluations. The results of LCT measurements and FEM simulations are compared and in very good agreement.

Acknowledgment

The authors would like to thank T. Jewula and H. Öztürk for helpful discussions and for providing the samples.

References

[1] B. Ivira, R. Fillit, P. Benech, F. Ndagijimana, G. Parat, and P. Ancey, "BAW resonators reliability in the GHz range," in *IEEE Industrial Electronics, IECON 2006 - 32nd Annual Conference on*, 2006, pp. 3133–3138.

[2] O. Wunnicke, P. van der Wel, R. Strijbos, and F. de Bruijn, "Thermal behavior of BAW filters at high RF power levels," *Ultrasonics, Ferroelectrics and Frequency Control, IEEE Transactions on*, vol. 56, pp. 2686–2692, 2009.

[3] D. Blackburn, "Temperature measurements of semiconductor devices - a review," in *Semiconductor Thermal Measurement and Management (SEMI-THERM) Symposium, 20th Annual IEEE*, 2004, pp. 70–80.

[4] P. R. N. Childs, J. R. Greenwood, and C. A. Long, "Review of temperature measurement," *Review of Scientific Instruments*, vol. 71, pp. 2959–2978, 2000.

[5] G. Aszódi, J. Szabon, I. Jánossy, and V. Székely, "High resolution thermal mapping of microcircuits using nematic liquid crystals," *Solid-State Electronics*, vol. 24, pp. 1127–1133, 1981.

[6] K. Azar, J. Benson, and V. Manno, "Liquid crystal imaging for temperature measurement of electronic devices," in *Semiconductor Thermal Measurement and Management (SEMI-THERM) Symposium, 7th Annual IEEE*, 1991, pp. 23–33.

[7] J. L. Fergason, "Liquid crystals in nondestructive testing," *Applied Optics*, vol. 7, pp. 1729–1737, 1968.

[8] C. R. Smith, D. R. Sabatino, and T. J. Praisner, "Temperature sensing with thermochromic liquid crystals," *Experiments in Fluids*, vol. 30, pp. 190–201, 2001.

[9] J. Hay and D. Hollingsworth, "A comparison of trichromic systems for use in the calibration of polymer-dispersed thermochromic liquid crystals," *Experimental Thermal and Fluid Science*, vol. 12, pp. 1–12, 1996.

[10] J. Hay and D. Hollingsworth, "Calibration of micro-encapsulated liquid crystals using hue angle and a dimensionless temperature," *Experimental Thermal and Fluid Science*, vol. 18, pp. 251–257, 1998.

[11] V. Kakade, G. Lock, M. Wilson, J. Owen, and J. Mayhew, "Accurate heat transfer measurements using thermochromic liquid crystal. Part 1: Calibration and characteristics of crystals," *International Journal of Heat and Fluid Flow*, vol. 30, pp. 939–949, 2009.

[12] Y. Rao and S. Zang, "Calibrations and the measurement uncertainty of wide-band liquid crystal thermography," *Measurement Science and Technology*, vol. 21, p. 015105, 2010.

[13] D. R. Sabatino, T. J. Praisner, and C. R. Smith, "A high-accuracy calibration technique for thermochromic liquid crystal temperature measurements," *Experiments in Fluids*, vol. 28, pp. 497–505, 2000.